THE COMMON LAND MODEL

BY YONGJIU DAI, XUBIN ZENG, ROBERT E. DICKINSON, IAN BAKER, GORDON B. BONAN, MICHAEL G. BOSILOVICH, A. SCOTT DENNING, PAUL A. DIRMEYER, PAUL R. HOUSER, GUOYUE NIU, KEITH W. OLESON, C. ADAM SCHLOSSER, AND ZONG-LIANG YANG

Scientists from several institutions and with different research backgrounds have worked together to develop a prototype modular land model for weather forecasting and climate studies. This model is now available for public use and further development.

Climate and weather forecasting models require the energy, water, and momentum fluxes across the land–atmosphere interface to be specified. Various land surface parameterizations (LSPs), ranging from the simple bucket-type LSP in the 1960s to the current soil–vegetation–atmosphere interactive LSP, have been developed in the past four decades to calculate these fluxes. The Project for Intercomparison of Land Surface Parameterization Schemes (PILPS) has demonstrated that, even with the same atmospheric forcing data and similar land surface parameters, different LSPs still give significantly different surface fluxes and soil wetness, partly because of the differences in the formulations of individual processes and coding architectures in participant models (Henderson-Sellers et al. 1995). On the other hand, most LSPs share many common components, suggesting the need to develop a publicly available common land model with a modular structure that could facilitate the exploration of new issues, less repetition of past efforts, and sharing of improvements and refinements contributed by different groups.

The Common Land Model (CLM) effort dates back to the mid-1990s and has evolved through various workshops and e-mail correspondence. The initial motivation was to provide a framework for a truly community-developed land component of the National Center for Atmospheric Research (NCAR) Community Climate System Model (CCSM). Interest in applying CLM came from the Goddard Space Flight Center (GSFC) Data Assimilation Office (DAO), which was implementing the Mosaic model (Koster and Suarez 1992), and the Center for Ocean–Land–Atmosphere Studies (COLA) scientists, who were revising their Simplified Simple Biosphere Model (SSiB) (Xue et al. 1991). We also established ties to groups performing carbon cycle and ecological modeling.

In developing CLM, we attempted to combine the best features of three existing successful and relatively

AFFILIATIONS: DAI AND DICKINSON—School of Earth and Atmospheric Sciences, Georgia Institute of Technology, Atlanta, Georgia; ZENG—Department of Atmospheric Sciences, University of Arizona, Tucson, Arizona; BAKER AND DENNING—Department of Atmospheric Sciences, Colorado State University, Fort Collins, Colorado; BONAN AND OLESON—National Center for Atmospheric Research, Boulder, Colorado; BOSSILOVICH AND HOUSER—NASA GSFC, Greenbelt, Maryland; DIRMEYER AND SCHLOSSER—Center for Ocean–Land–Atmosphere Studies, Calverton, Maryland; NIU AND YANG—Department of Geological Sciences, University of Texas at Austin, Austin, Texas
CORRESPONDING AUTHOR: Dr. Yongjiu Dai, School of Earth and Atmospheric Sciences, Georgia Institute of Technology, 311 Ferst Dr., Atlanta, GA 30332
E-mail: dai@eas.gatech.edu
DOI: 10.1175/BAMS-84-8-1013

In final form 4 February 2003
©2003 American Meteorological Society

well documented and modular land models; the Land Surface Model (LSM) of Bonan (1996), the Biosphere–Atmosphere Transfer Scheme (BATS) of Dickinson et al. (1993), and the 1994 version of the Chinese Academy of Sciences Institute of Atmospheric Physics LSM (IAP94) (Dai and Zeng 1997). However, CLM is designed in such a way that model components from other LSPs can be incorporated into it very easily. Since the initial CLM code was completed in late 1998, the FORTRAN90 program has gone through four iterations of improvements. Since then CLM has also gone through four rigorous beta tests. We have used very comprehensive observational data: a variety of multiyear point observational data over different regions of the world, regional data over the U.S. Red–Arkansas River basin, and the Global Soil Wetness Project (GSWP) (Dirmeyer et al. 1999) data. These data include all data in PILPS. CLM has also been tested in the multiagency Land Data Assimilation System (LDAS). Results from these extensive tests will be published elsewhere by CLM participants. In addition, CLM has been coupled with the NCAR Community Climate Model (CCM3) (Zeng et al. 2002). The results of this coupled run have shown that CLM simulates surface air temperature, the annual cycle of runoff, and snow mass significantly better than the LSM.

The overall structure of CLM includes three elements: 1) the core single-column soil–snow–vegetation biophysical code, 2) the land boundary data, and 3) the scaling procedures within a climate model required to interface atmospheric model grid-square inputs to land single-column processes. The interface routines that isolate the land model from the needed data structures are also important. Such separation of functionality allows the best science to be used for each of these elements, and, in particular, ensures that the core model can be tested with single-point field data, that the latest satellite remote sensing and global field survey datasets can be incorporated, and that the latest scaling procedures can be adopted. This paper primarily documents the single-column model treatment and some of the offline testing results. Two initial versions of land boundary data have been documented in Zeng et al. (2002) and Bonan et al. (2002).

CLM has added complexity in order to satisfy a wide variety of applications. For example, the multilayer soil and snow structure provides accurate simulations over a wide variety of timescales and hence is useful for such disparate applications as model data assimilation of surface properties, and determining soil temperatures beneath snow for matching measurements of soil respiration. Managing such complexity is not easy. However, we anticipate that good documentation and the open scrutiny of many scientists will eliminate any serious errors. Simplified versions for specific applications would not be difficult to develop. However, further improvements in the parameterization of runoff, and better integration into models of vegetation dynamics and soil biogeochemistry, are likely to further increase the code complexity.

In this article, we will first describe in brief the model initialization needs and physical parameterizations and then report some encouraging offline model testing results using two observational datasets.

INPUT DATA REQUIREMENTS. With the tremendous advances made recently in observational technology and environmental databases, there are many land surface characteristics datasets available for land surface modeling. CLM is designed to handle a variety of data sources. To take advantages of different datasets in CLM, preprocessing of data is necessary. This includes land surface type, soil and vegetation parameters, model initialization, and atmospheric boundary conditions.

Land surface characteristics. Three indexes are used to define land surface characteristics: land cover type, soil texture, and soil color. In general, any classification of land cover, soil texture, and soil color could be implemented within CLM. As defaults, the land cover types are based on the International Geosphere–Biosphere Programme (IGBP) classification system, soil color is the same as in BATS, and soil texture is the same as in LSM (by percentages of sand and clay).

Vegetation and soil properties. CLM contains both time-invariant and time-varying vegetation parameters. The former consists of morphological parameters (canopy roughness, zero-plane displacement, leaf dimension, and rooting depths), optical properties (albedos of thick canopy), and physiological properties that are mainly related to the functioning of the photosynthesis–conductance model. The latter includes green leaf area index (L_{AI}) and stem area index, including dead leaf or litter (S_{AI}).

The soil thermal and hydraulic parameters—specific heat capacity of dry soil, thermal conductivity of dry soil, porosity, saturated negative potential, saturated hydraulic conductivity, and the exponent B defined in Clapp and Hornberger (1978)—are derived from depth-varying percentages of sand and clay, as in LSM. The estimation of soil parameters is critically important in land surface modeling (Duan et al.

2001). Even though the current setup of CLM determines soil parameters a priori based on LSM experience, users of CLM can assign different values based on their own experience. Recent studies indicated that the use of multicriteria optimization procedures to adjust model parameters could lead to more realistic simulation of surface energy fluxes (Gupta et al. 1999; Bastidas et al. 2003).

Model initialization. The model state variables that require initialization include canopy temperature, canopy interception water storage, temperature at the nodes of soil and snow layers, mass of water within the layer of soil and snow, mass of ice within the layer of soil and snow, and snow layer thickness. Ideally CLM is initialized using observed initial land states. The multiagency LDAS project has worked toward improving initial land state variables by driving LSPs with observed meteorological forcing data, and the model state variables can be used to run a weather/climate model for subsequent time periods. In the current CLM setup, atmospheric forcing data over an annual cycle are used to spin up the model to an equilibrium state, and variables at the equilibrium state are then taken as the initial values for a model simulation. For offline simulations, atmospheric forcing data includes wind speed, air temperature, and specific humidity of the atmosphere at some height or heights; precipitation rate; visible (beam and diffuse) and near-infrared (beam and diffuse) incident solar radiation; incident atmospheric longwave radiation; and surface pressure.

PHYSICAL AND NUMERICAL DESCRIPTIONS. This section briefly describes the parameterization of physical and biophysical processes in a vertical column and numerical schemes for solving the governing equations in CLM. With its modular structure, the treatment of individual processes in the CLM code can be easily revised or replaced by users. A simple representation of horizontal vegetation heterogeneity is also presented; this also can be easily replaced by users.

Horizontal and vertical representations. Every surface grid cell can be subdivided into any number of tiles, and each tile contains a single land cover type. This follows the general mosaic concept of Avissar (1992) and Koster and Suarez (1992). Energy and water balance calculations are performed over each tile at every time step, and each tile maintains its own prognostic variables. The tiles in a grid square respond to the mean conditions in the overlying atmospheric grid box, and this grid box, in turn, responds to the areally weighted fluxes of heat and moisture from the tiles. The tiles within a grid square do not interact with each other directly.

CLM has one vegetation layer, and multiple unevenly spaced vertical soil layers and snow layers, optimized to reproduce higher-resolution calculation of diurnal and seasonal temperature variations in all layers. The indexing for snow layers permits the accumulation or ablation of snow at the top of the snow cover without renumbering the layers, and the number of snow layers could be changed with the total snow depth.

Time-integration scheme. Time integration proceeds by a split-hybrid scheme, where the solution procedure is split into "energy balance" and "water balance" phases in a very modularized structure. Energy and water are conserved at each time step.

Surface albedo. The canopy albedo treatment has been developed to capture the essential features of a two-stream radiative transfer model while forgoing the complexity of the full treatment. It combines soil and canopy albedos by simple rules that reduce toward correct asymptotic limits for thick and thin canopies and provide reasonable results for intermediate values of leaf area index. Yang et al. (1999a) assessed the simulations using this method within BATS and found that the resulting ground heat fluxes are comparable to those from IAP94, which uses a two-stream radiative transfer model. The current treatment of soil and snow in CLM is directly adopted from BATS. Soil albedos are a function of soil color and moisture in the surface soil layer. Snow albedos are inferred from the calculations of Warren and Wiscombe (1980) and the snow model and data of Anderson (1976), and they are a function of snow age, grain size, solar zenith angle, pollution, and the amount of fresh snow. Over a snow-covered tile, the surface albedo is estimated by a linear combination of albedos for snow and canopy plus soil.

Turbulent fluxes. The turbulent eddy fluxes are proportional to quantity differences multiplied by a conductance. The conductances (or inverse resistances) are considered over pathways between the canopy and the atmospheric height, within the canopy, and between the canopy and ground. The vector momentum fluxes, the sensible heat flux, and the water vapor flux between the atmosphere at reference height and the canopy top (or bare ground) are derived from the Monin–Obukhov similarity theory, which is solved by

an iterative numerical method (Zeng et al. 1998). The leaf laminar boundary layer resistance for heat and vapor within the canopy, and the aerodynamic resistance below the canopy, are directly adopted from BATS.

Surface evapotranspiration consists of evaporation from wetted stems and leaves E_w, transpiration through the plant E_{tr}, and initial evaporation from the ground (i.e., bare soil or snow surfaces) E_g. The equations for E_w and E_{tr} are similar to those used in BATS, while Philip's (1957) formulation is used for the computation of E_g. The stomatal resistance in the formulation of E_{tr} is directly adopted from LSM.

Photosynthesis and stomatal resistance. The leaf assimilation (or gross photosynthetic) rate is described as approaching the minimum of three limiting rates: the assimilation rate as limited by the efficiency of the photosynthetic enzyme system (Rubisco limited), the amount of photosynthetically active radiation (PAR) captured by the leaf chlorophyll, and the capacity of the leaf to export or utilize the products of photosynthesis. The leaf photosynthesis and conductance are linked by the semiempirical equation of Ball (see Sellers et al. 1996). In this equation, the partial pressures of CO_2 and the leaf surface relative humidity are determined from conditions in the canopy air space through leaf conductance, the leaf-boundary-layer conductance, the net flux of CO_2, and leaf transpiration. The complete equation set can be solved to yield mutually consistent values of leaf photosynthesis and transportation (Bonan 1996). The photosynthesis equations are solved both for sunlit and shaded leaves by using their respective canopy averages of the amount of PAR they absorb. The averages of conductance and canopy photosynthesis are weighted by the fractions and leaf area indices of the sunlit and shaded leaves.

TEMPERATURES. *Leaf temperature.* The foliage is assumed to have zero heat capacity, and photosynthetic and respiratory energy transformations are neglected. Foliage energy conservation then yields

$$R_{n,c} - H_c - L_v E_c = 0, \tag{1}$$

where $R_{n,c}$ is the net radiation absorbed by canopy, and H_c and LE_c are, respectively, the sensible and latent heat fluxes from the leaves. This equation is solved for canopy temperature by the Newton–Raphson iteration method, which at each iteration includes the calculation of the photosynthesis and stomatal resistance, and the integration of turbulent flux profiles. The air within the canopy has negligible heat and water vapor capacities, so heat and water vapor fluxes from the foliage and from the ground must be balanced by heat and water vapor fluxes to the atmosphere.

Snow and soil temperatures. The soil (or snow) heat transfer is assumed to obey the following heat diffusion equation:

$$c\frac{\partial T}{\partial t} = -\frac{\partial F}{\partial z} + S, \tag{2}$$

where c is the volumetric heat capacity and is calculated as a linear combination in terms of the volumetric fraction of the constituent phases, T is the temperature, z is the vertical coordinate (distance from soil surface, positive downward), S is the latent heat of phase change, and F is heat flux. The subsurface heat flux F at depth z can be described by the Fourier law for heat conduction:

$$F = -\lambda\frac{\partial T}{\partial z}, \tag{3}$$

where λ is the thermal conductivity as computed using the algorithm of Johansen (as reported by Farouki 1982) for soil or using the formulation of Jordan (1991) for snow. The heat flux F at the surface is taken as

$$F = R_{n,g} - H_g - LE_g, \tag{4}$$

where $R_{n,g}$ is the net radiation absorbed by ground surface, and H_g and LE_g are, respectively, the sensible and latent heat fluxes. The heat flux is assumed to be zero at the bottom of the soil column.

Soil/snow temperature is predicted from Eq. (4) for unevenly spaced soil layers and up to a maximum value of snow layers. The thermal conductivities at the interfaces between two neighboring layers (i, $i + 1$) are derived based on the constraint that the flux across the interface is equal to that from the node i to the interface and the flux from the interface to the node $i + 1$. Using the Crank–Nicholson numerical scheme, the temperature equation is reduced to a tridiagonal system.

Phase change. To numerically solve the heat equation, the temperature profile is calculated without the phase change term and then readjusted for phase change. The readjustment involves three steps: 1) the temperatures are reset to the freezing point for layers

undergoing phase change when the layer temperature is greater than the freezing point and the ice mass is not equal to zero (i.e., melting), or when the layer temperature is less than the freezing point and the liquid water mass is not equal to zero (i.e., freezing); 2) the rate of phase change is assessed from the energy excess (or deficit) resulting from adjusting layer temperature to freezing point; and 3) the ice and liquid mass and the layer temperature are readjusted.

WATER BALANCE. *Canopy water storage.* Canopy water is a simple mass balance determined by gains from interception of precipitation and dew condensation and loss from evaporation; that is,

$$\frac{\partial w_{\text{dew}}}{\partial t} = \sigma_f P - D_d - D_r - E_w. \tag{5}$$

Precipitation P arriving at the vegetation top is either intercepted by foliage or directly falls through the gaps of leaves to ground. The parameterization of direct throughfall D_d is similar to that of the transmission of solar beam for spherically distributed leaves. The canopy drip D_r (outflow of the water stored on foliage and stem) occurs when water storage is greater than the maximum holding capacity. Evaporation E_w from the wet canopy is parameterized as the local potential evaporation, and σ_f is the vegetation fraction cover not buried by snow.

Snow water. Water flow is computed by a simple explicit scheme that permits a portion of liquid water over the holding capacity of snow to percolate into the underlying layer. When the porosity of one of the two neighboring layers is less than 0.05, however, water flow is assumed to be zero. The water flow out of the bottom of the snowpack is available for infiltration into the soil and runoff.

Soil moisture. The vertical soil moisture transport is governed by infiltration, runoff, gradient diffusion, gravity, and soil water extraction through roots for canopy transpiration. The equations for liquid soil water and soil ice can be written as

$$\frac{\partial w_{\text{liq}}}{\partial t} = -\frac{\partial q}{\partial z} - f_{\text{root}} E_{\text{tr}} + M_{\text{il}}, \tag{6}$$

$$\frac{\partial w_{\text{ice}}}{\partial t} = -M_{\text{il}} - M_{\text{iv}}, \tag{7}$$

where w_{liq} is the mass of soil water, f_{root} is the root fraction, M_{il} is the mass rate of melting (positive) or freezing (negative) of soil ice, M_{iv} is the mass rate of sublimation of soil ice, and q is the water flow. The vertical water flow within soil is described by Darcy's law,

$$q = -K\left[\frac{\partial \psi}{\partial z} - 1\right], \tag{8}$$

and the hydraulic conductivity K and the soil negative potential ψ vary with soil water content and soil texture based on Clapp and Hornberger (1978) and Cosby et al. (1984). The net water flux applied to the surface layer is provided by snowmelt, precipitation, and throughfall of canopy dew, minus surface runoff and evaporation:

$$q = \begin{cases} (1-\sigma_f)P + D_d + D_r - E_g - R_s, & \textit{for nonsnow-covered soil} \\ S_m - R_s, & \textit{for snow-covered soil} \end{cases}, \tag{9}$$

where S_m is the rate of snowmelt, E_g is the evaporation from soil, and R_s is the surface runoff.

Soil moisture is predicted from an unevenly spaced layers model (as with soil temperatures). Equation (8) is integrated over the layer thickness in which the temporal variation in water mass must equal the net flow across the bounding interfaces, plus the rate of internal source or sink. The terms of water flow across the layer interfaces are linearly expanded using a first-order Taylor expansion. The equations result in a tridiagonal system. Equation (9) is solved by an explicit method.

Runoff. Model runoff includes surface and base flow, both of which are computed over saturated and unsaturated areas separately. The fraction of the saturated area depends on the soil moisture state, represented by a nondimensional water table depth and topographic features (currently assumed to be a constant parameter). Surface runoff is parameterized as

a combination of Dunne runoff (saturation excess runoff) in the saturated fraction and BATS-type surface runoff; the latter is proportional to the surface soil moisture state, in the unsaturated fraction. The formation of base flow contains three different mechanisms: bottom drainage, saturation excess, and lateral subsurface runoff due to local slopes.

Snow compaction. Three mechanisms for of changing snow characteristics are implemented: destructive, overburden, and melt. The treatments of the first two are from Jordan (1991), while the contribution due to melt metamorphism is simply taken as a ratio of snow ice fraction after melting to that before melting.

CLM OFFLINE TESTS. As mentioned earlier, we have done extensive offline tests using a variety of observational data. These tests have demonstrated that CLM can reasonably simulate land surface processes. Detailed discussion of these tests will be presented in a separate paper. Results from the coupling of CLM with the NCAR CCM3 have further demonstrated that, compared with the original NCAR land surface model, CLM significantly improves the climate simulation of surface air temperature and the overall hydrological cycle (Zeng et al. 2002). Here, just as an example, we show results from two offline tests with different sets of observation, one from a grassland meadow and the other from the Brazilian rainforest. Results from BATS, LSM, and IAP94 are shown for comparison.

For each run, the atmospheric forcing data for the first year are used for model spinup with soil water initialized at full saturation, soil temperature equal to air temperature, and both snow depth and snow age at zero. The equilibrium, as defined by Yang et al. (1995), is reached in typically 10 yr or less, and variables at the end of the spinup process then serve as the initial values for CLM offline simulations.

Valdai. The Valdai dataset was one of those used in PILPS [Phase 2(d)] for land model intercomparison studies (Vinnikov et al. 1996; Schlosser et al. 1997, 2000). It contains a continuous 18-yr time series (1 January 1996–31 December 1983) of atmospheric forcing and hydrological data for a grassland meadow (57°58′N, 33°14′E). The atmospheric forcing data were originally sampled at 3-h intervals but were interpolated to 30-min intervals for land modeling. Incident solar radiation and downward longwave radiation were not measured, and hence were estimated using empirical algorithms.

For our test, the models are set up largely following the instructions for PILPS 2(d) (Schlosser et al. 2000). The grid is assumed to consist of two patches: 90% grassland and 10% bare soil. The soil texture types for the top 1 m of soil are converted into the percentages of sand and clay using Table 2 of Cosby et al. (1984) for model soil layers. A high value of clay was assumed for the soil deeper than 1 m (47% clay and 6% sand).

CLM simulates very well the overall seasonal and interannual variability of snow water equivalent depth (SWE), and accurately simulates the beginning of accumulation and the ending of ablation over all 18 yr observed (Fig. 1). Similar to most PILPS models (Slater et al. 2001), CLM simulates less SWE over two winters (1967/68 and 1968/69), and simulates excessive SWE in most others thereafter. The CLM, BATS, and IAP94 models agree in their maximum SWE, length of snow season, and their discrepancies in midseason ablation. Issues pertaining to the simulated SWE from CLM, BATS, IAP94, and LSM, and, in

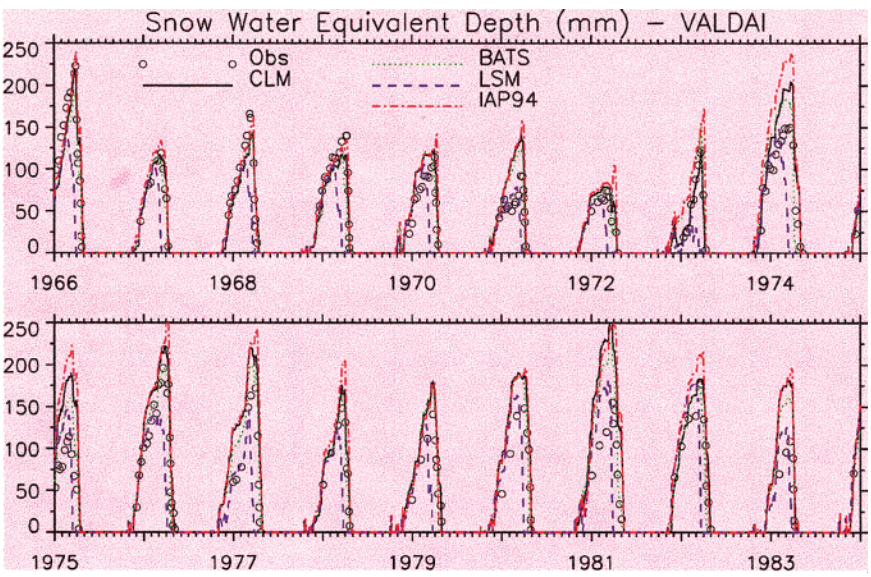

Fig. 1. Daily mean simulated and observed snow water equivalent depth (SWE) for 1966–83 for the Valdai catchment. The observational values represent the catchment-averaged SWE based on snow course measurements that resulted in up to 44 individual measurements throughout the catchment.

particular, the performance of CLM against observations have been addressed in previous analyses of Slater et al. (2001) and Yang et al. (1999b). Subsequent testing and development of CLM will carefully consider these issues. Nevertheless, the performance of CLM on the whole is quite comparable to the other three models (BATS, IAP94, and LSM) considered in this testing, as well as to the participating PILPS 2(d) models (e.g., Figs. 6–9 of Schlosser et al. 2000).

Overall, CLM reproduces the observed seasonal and interannual variability of soil water (Fig. 2). CLM produces drier than normal conditions for the dry summer of 1972 (although to a lesser degree than observed), but it fails to reproduce dry conditions in the fall of 1975. Most of the participating models in PILPS 2(d) had difficulty in reproducing the fall drought of 1975 (discussed in Schlosser et al. 2000), however. CLM's underestimation of these low-soil-moisture events can be attributed in part to CLM's depiction of its deep soil layers, which are assumed to have higher clay contents, and hence lower conductivity, higher soil suction, and higher soil volumetric content at wilting point. In addition, the assumed zero water holding capacity of frozen soil (Fuches et al. 1978) may also contribute to CLM's consistent underestimation of wintertime soil moisture conditions.

As it does for the SWE and soil moisture, CLM realistically simulates the seasonal and interannual variability of runoff (Fig. 3). The runoff peaks in spring are well captured and consistent with the snowmelt in Fig. 1. However, CLM overpredicts the runoff in most of the growing seasons and underpredicts it in the fall. The models considered here generally overestimate runoff in the growing seasons, however.

Observations show that, because the 1971/72 winter season had less snow cover and hence lower insulation than the 1979/80 winter, it had a deeper frozen zone and lower soil temperature. CLM realistically reproduces these differences (Fig. 4), even

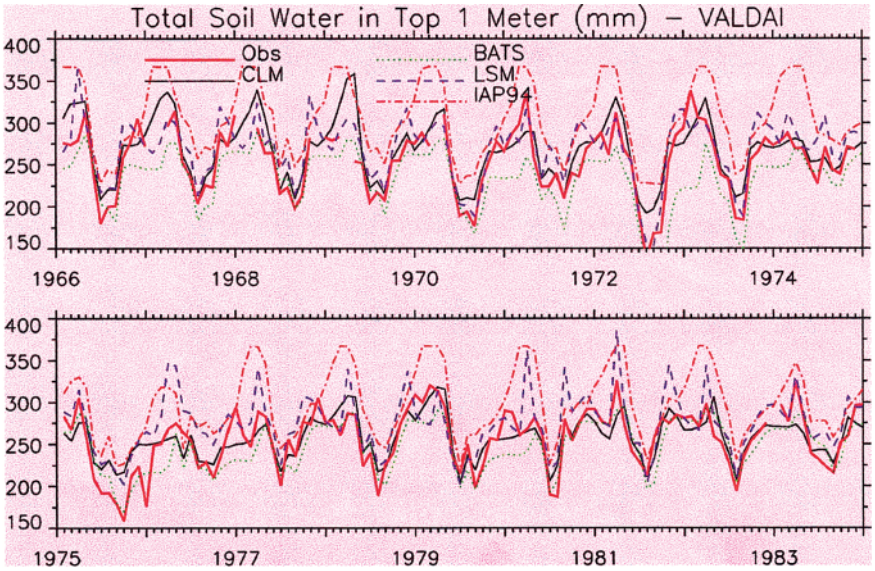

Fig. 2. Simulated and observed soil moisture in the top 1 m for the end day of each month for 1966–83 for the Valdai catchment. The observational values represent catchment-averaged soil water measured by the gravimetric method at the end of each month from 9 to 11 sites distributed over the catchment (Vinnikov et al. 1996).

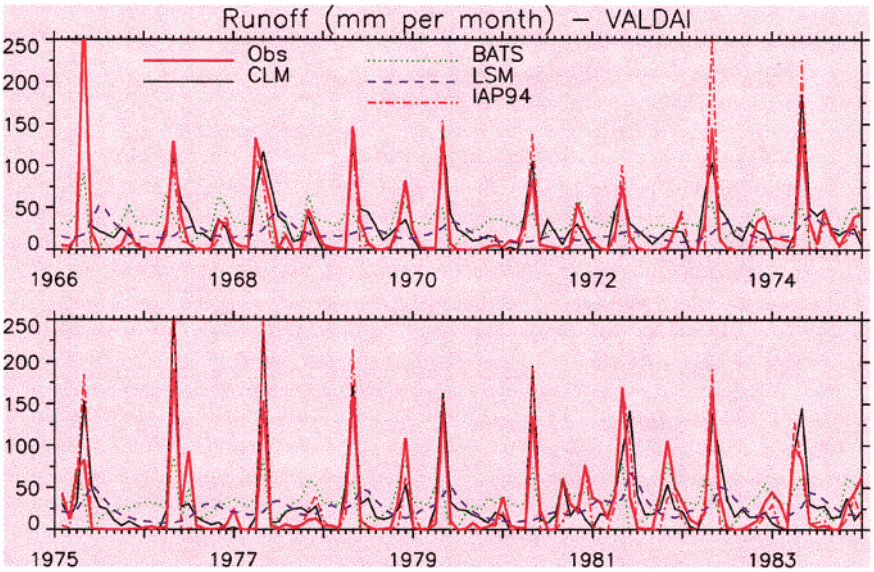

Fig. 3. Monthly mean simulated and observed runoff for 1966–83 for the Valdai catchment. Monthly runoff measurement were obtained by weir observations made at the outflow point of the catchment region (Schlosser et al. 1997).

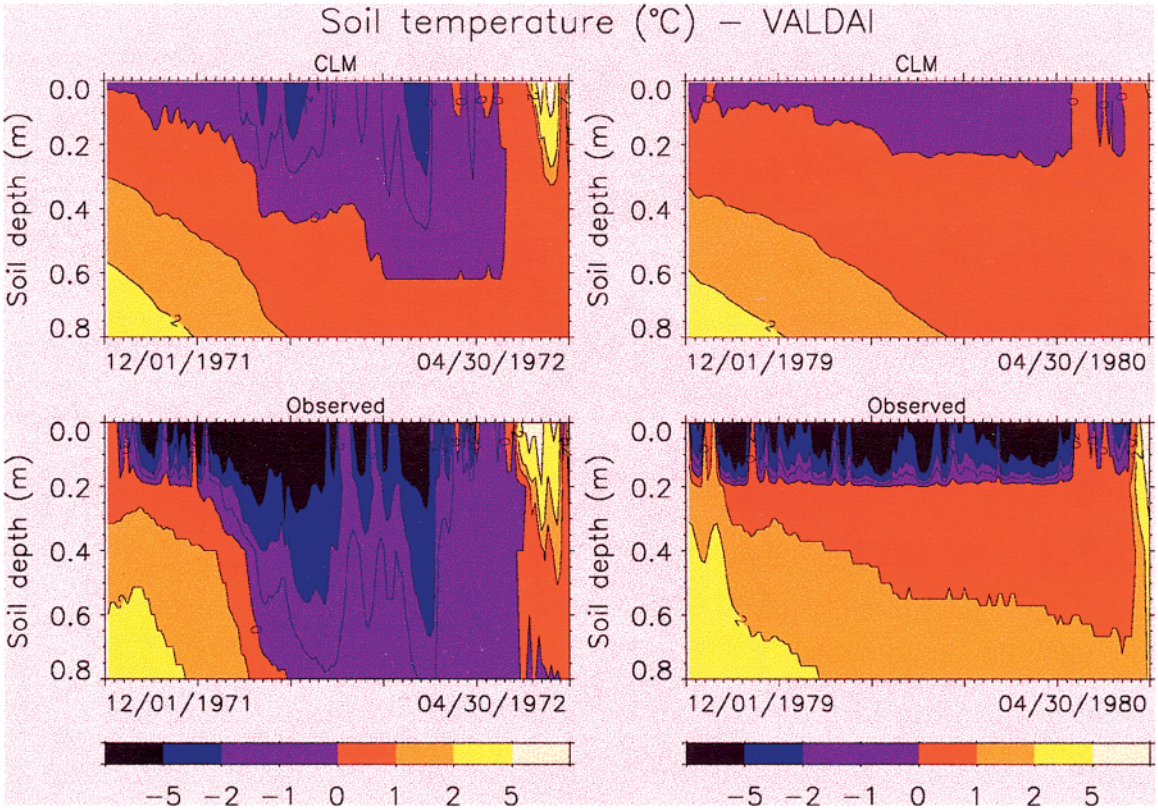

Fig. 4. Simulated and observed vertical distribution of soil temperature from 1 Dec to 30 Apr in 1971/72 and 1979/80 for the Valdai catchment. The simulations are daily averages. Observations were made once a day by thermometer at the surface and at 20-, 40-, and 80-cm depth.

though its frozen soil depth is shallower for 1971/72. The thermal conductivity λ and capacity $\rho_s c_p$ used in CLM are in normal ranges ($\lambda \sim 1.2$ to 3.0 W m^{-1}K^{-1} for unfrozen and frozen soils, respectively, and $\lambda \sim 0.1$ to 1.1 W m^{-1}K^{-1} for snow; $\rho_s c_p \sim 1.6 \times 10^6$ to 2.5×10^6 J m^{-3}K^{-1} for frozen and unfrozen soils, respectively, and $\rho_s c_p \sim 0.1 \times 10^6$ J m^{-3}K^{-1} for snow). Therefore, the shallower frozen soil depth in CLM might be related to the fact that the soil temperature was measured once a day (in contrast to the diurnal average in the model) by putting a thermometer into the ground at the surface (half buried horizonally), at depths of 20, 40, 80, and 120 cm. When the soil was covered by snow, the thermometer was put on the snow surface (K. Ya. Vinnikov and A. Robock 2002, personal communication).

ABRACOS. The second test involved data from the Anglo-Brazilian Amazonian Climate Observation Study (ABRACOS) that were collected at Reserva Jaru (10°05′S, 61°55′W) in the southwestern Amazon rainforest (Gash et al. 1996). Here, we used atmospheric forcing data for 2 yr (January 1992–December 1993). The forcing data do not include the downward longwave radiation but do have the net radiation. Turbulent flux observations are available for September 1992 (wet season) and June 1993 (dry season), while soil moisture was measured on a weekly basis at depths of 0.1 and 0.2 m, and then every 0.2 m down to 3.6 m during the whole period.

The site is classified as broadleaf evergreen forest with 100% cover. The monthly index of green leaf area index is derived from Advanced Very High Resolution Radiometer (AVHRR) data (Zeng et al. 2000). Other vegetation parameters are set at the models' default values for evergreen broadleaf forest. For CLM, we based the variation of soil texture with depth on Wright et al. (1996). The soil parameters for the other three models are the values for CLM at 0.4–0.6-m depth. From a depth of about 2 m, the soil merges downward into saprolite, then into fairly hard weathered granite. The bottom of the soil column for all four models is taken as granite bedrock without drainage (i.e., hydraulic conductivity at saturation $K_{sat} = 0$).

For September 1992 (a dry month), all models realistically simulate latent heat fluxes, while sensible heat fluxes simulated in CLM are closer to observa-

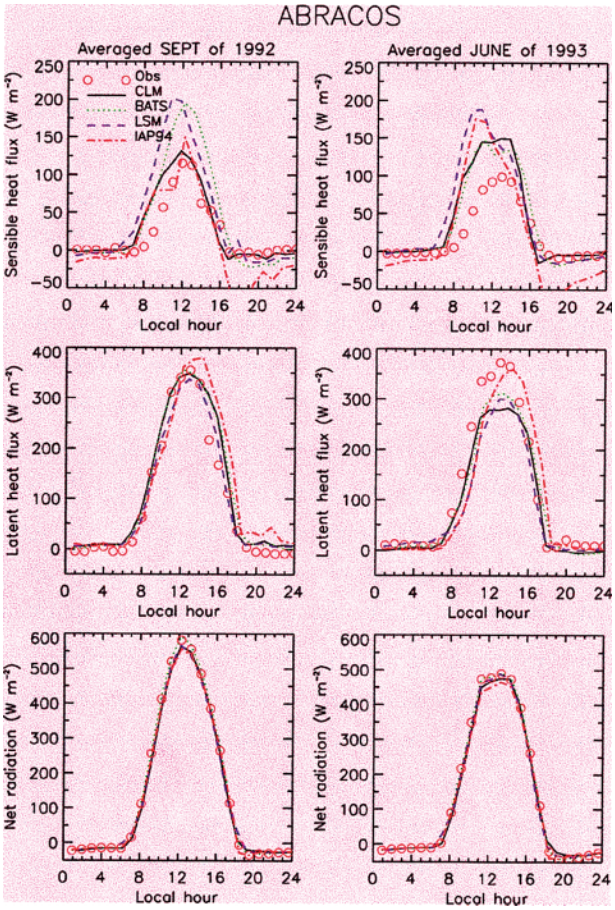

Fig. 5. Simulated and observed diurnal cycle of energy fluxes (net radiation, and latent and sensible heat fluxes) over two periods for the ABRACOS forest site in southwestern Amazonia, averaged over (left) Sep 1992 and (right) Jun 1993.

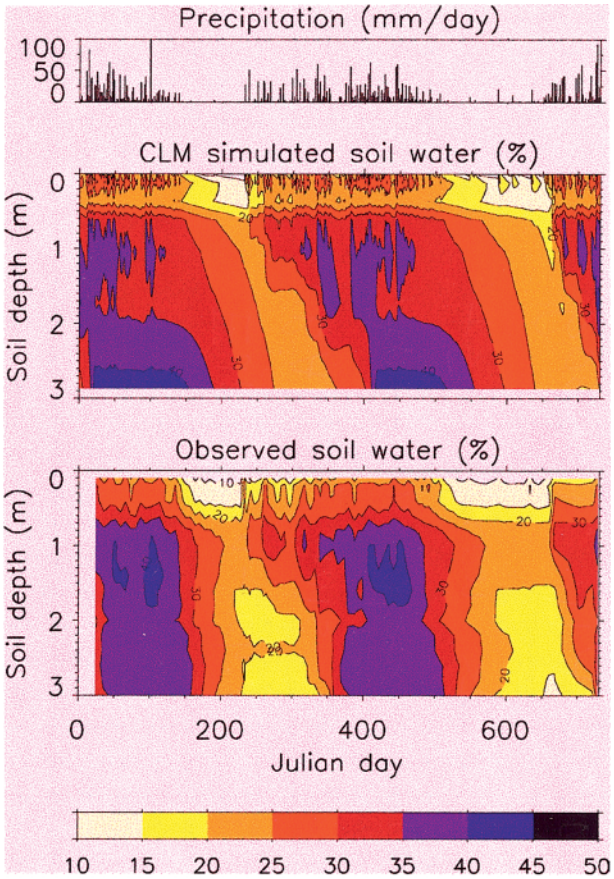

Fig. 6. Seasonal variations of precipitation and soil moisture over the years 1992 and 1993 for the ABRACOS forest site in southwestern Amazonia. The simulations of soil moisture are daily averages, and observations of soil moisture are measured once a week.

tions (Fig. 5). In June 1993 (a wet month), CLM overestimates the peak values of sensible heat fluxes and underestimates latent heat fluxes. Not surprisingly, all models tested realistically simulate the net radiation R_n, because the observed R_n data were used indirectly to obtain the diurnal longwave radiation.

The seasonal variation of soil moisture at different depths has not been widely studied before because of limited observations and the few soil layers of most land models. CLM realistically simulates the alternating wet and dry periods in the top 50 cm (Fig. 6). Deep soil in the model, however, is wetter than indicated by observations during the dry season, probably because of the assumption of soil column bottom at bedrock in the model.

SUMMARY. More than 30 land surface models have been published so far, and this number increases every year. This emphasis reflects the general recognition of the importance of land surface processes in weather forecasting and climate studies. These models share many common components with each other. However, even with the same atmospheric forcing data and similar land surface parameters, these models still give significantly different surface fluxes and soil wetness.

While individual land model development (particularly with innovation) should be always encouraged, scientists from several institutions also recognized a few years ago that some synergy and model convergence are also needed. The Common Land Model (CLM), presented in this paper, represents our efforts in this direction. Offline studies presented here demonstrate that CLM can realistically simulate the key state variables and fluxes. Confirmation of the results using other observational datasets will be reported elsewhere. Furthermore, when CLM is coupled with the NCAR CCM3, it is found to significantly improve the climate simulation of surface air temperature, runoff, and snow mass, with little im-

pact on other aspects (Zeng et al. 2002). Therefore, CLM is now ready for public release (Dai et al. 2001).

Some of the components in CLM need to be further improved. For instance, the runoff parameterization follows the ideas of TOPMODEL, but subgrid topographic data have not been used. The interaction of underground water with the surface water has not been considered either. Primarily as a biophysical model, the biogeochemical cycle and dynamic vegetation components also need to be added to CLM. The modular code structure of CLM would help facilitate these improvements and further developments by the larger community.

ACKNOWLEDGMENTS. The development of CLM was supported by multiple funding agencies, including NASA, NSF, NOAA, and DOE. In particular, the first three authors were primarily supported by the NASA EOS/IDS Program. We would like to acknowledge the assistance and helpful discussions from J. Radakovich, J. Entin, and S. Sorooshian's group. We would also like to thank Dr. Qingyun Duan for his thorough and constructive review. We appreciate valuable comments by three anonymous reviewers. The evaluation described in this paper would not have been possible without the generous support of a number of experimental groups. The Valdai data were made available by A. Robock at The State University of New Jersey at Rutgers, K. Vinnikov at the University of Maryland, C. A. Schlosser at COLA, and N. A. Speranskaya at the State Hydrological Institute at Russia; the ABRACOS data were collected under the ABRACOS project and made available by the Institute of Hydrology (United Kingdom) and the Instituto Nacional de Pesquisas Espaciais (Brazil).

REFERENCES

Anderson, E. A., 1976: A point energy and mass balance model of a snow cover. NOAA Tech. Rep. NWS 19, Office of Hydrology, National Weather Service, Silver Spring, MD, 150 pp.

Avissar, R., 1992: Conceptual aspects of a statistical–dynamical approach to represent the landscape subgrid-scale heterogeneities in atmospheric models. *J. Geophys. Res.,* **97** (D3), 2729–2742.

Bastidas, A. L., H. V. Gupta, K.-L. Hsu, and S. Sorooshian, 2003: Parameter, structure, and model performance evaluation for land surface schemes. *Calibration of Watershed Models,* Q. Duan and J. N. Almonte, Eds., Water Science and Applications Series 6, Amer. Geophys. Union, 229–237.

Bonan, G. B., 1996: A land surface model (LSM version 1.0) for ecological, hydrological, and atmospheric studies: Technical description and user's guide. NCAR Tech. Note NCAR/TN-417+STR, 150 pp.

——, K. W. Oleson, M. Vertenstein, S. Levis, X. Zeng, Y. Dai, R. E. Dickinson, and Z.-L. Yang, 2002: The land surface climatology of the community land model coupled to the NCAR community climate model. *J. Climate,* **15,** 3123–3149.

Clapp, B. J., and G. M. Hornberger, 1978: Empirical equations for some soil hydraulic properties. *Water Resour. Res.,* **14,** 601–604.

Cosby, B. J., G. M. Hornberger, R. B. Clapp, and T. R. Ginn, 1984: A statistical exploration of the relationships of soil moisture characteristics to the physical properties of soils. *Water Resour. Res.,* **20,** 682–690.

Dai, Y., and Q.-C. Zeng, 1997: A land surface model (IAP94) for climate studies, Part I: Formulation and validation in off-line experiments. *Adv. Atmos. Sci.,* **14,** 433–460.

——, and Coauthors, cited 2001: Common Land Model: Technical documentation and user's guide. [Available online at http://climate.eas.gatech.edu/dai/clmdoc.pdf.]

Dickinson, R. E., A. Henderson-Sellers, P. J. Kennedy, and M. F. Wilson, 1993: Biosphere–Atmosphere Transfer Scheme (BATS) version 1e as coupled to Community Climate Model. NCAR Tech. Note NCAR/TN-387+STR, 72 pp.

Dirmeyer, P. A., A. J. Dolman, and N. Sato, 1999: The Global Soil Wetness Project: A pilot project for global land surface modeling and validation. *Bull. Amer. Meteor. Soc.,* **80,** 851–878.

Duan, Q., J. Schaake, and V. Korem, 2001: A priori estimation of land surface model parameters. *Land Surface Hydrology, Meteorology and Climate: Observations and Modeling,* V. Lakshmi, J. Albertson, and J. Schaake, Eds., Water Science and Applications Series, 3, Amer. Geophys. Union, 77–94.

Farouki, O. T., 1982: *Thermal Properties of Soils. CRREL Monogr.,* No. 81-1, U.S. Army Cold Regions Research and Engineering Laboratory, 136 pp.

Fuchs, M., G. S. Campbell, and R. I. Papendick, 1978: An analysis of sensible and latent heat flow in a partially frozen unsaturated soil. *Soil Sci. Soc. Amer. J.,* **42,** 379–385.

Gash, J. H. C., C. A. Nobre, J. M. Roberts, and R. L. Victoria, 1996: An overview of the Anglo-Brazilian Amazonian Climate Observation Study (ABRACOS). *Amazonian Deforestation and Climate,* J. H. C. Gash, et al., Eds., John Wiley and Sons, 1–14.

Gupta, H. V., L. A. Bastidas, S. Sorooshian, W. J. Shuttleworth, and Z. L. Liang, 1999: Parameter estimation of a land surface scheme using multi-criteria methods. *Geophys. Res.,* **104**(D16), 19 491–19 504.

Henderson-Sellers, A., A. J. Pitman, P. K. Love, P. Irannejad, and T. Chen, 1995: The Project for Intercomparison of Land Surface Parameterisation Schemes (PILPS) Phases 2 and 3. *Bull. Amer. Meteor. Soc.,* **76,** 489–503.

Jordan, R., 1991: A one-dimensional temperature model for a snow cover: Technical documentation for SNTHERM.89. U.S. Army Cold Regions Research and Engineering Laboratory Special Rep. 91-16, 49 pp.

Koster, R. D., and M. J. Suarez, 1992: Modeling the land-surface boundary in climate models as a composite of independent vegetation stands. *J. Geophys. Res.,* **97**(D3), 2697–2715.

Philip, J. R., 1957: Evaporation and moisture and heat fields in the soil. *J. Meteor.,* **14,** 354–366.

Schlosser, C. A., A. Robock, K. Ya. Vinnikov, N. A. Speranskaya, and Y. Xue, 1997: 18-year land-surface hydrology model simulations for a midlatitude grassland catchment in Valdai, Russia. *Mon. Wea. Rev.,* **125,** 3279–3296.

——, and Coauthors, 2000: Simulation of a boreal grassland hydrology at Valai, Russia: PILPS phase 2(d). *Mon. Wea. Rev.,* **128,** 301–321.

Sellers, P. J., and Coauthors, 1996: A revised land surface parameterization (SiB2) for atmospheric GCMs. Part I: Model formulation. *J. Climate,* **9,** 676–705.

Slater, A. G., and Coauthors, 2001: The representation of snow in land surface schemes: Results from PILPS 2(d). *J. Hydrometeor.,* **2,** 7–25.

Vinnikov, K. Ya., A. Robock, N. A. Speranskaya, and C. A. Schlosser, 1996: Scales of temporal and spatial variability of midlatitude soil moisture. *J. Geophys. Res.,* **101,** 7163–7174.

Warren, S. G., and W. J. Wiscombe, 1980: A model for the spectral albedo of snow. II: Snow containing atmospheric aerosols. *J. Atmos. Sci.,* **37,** 2734–2745.

Wright, I. R., and Coauthors, 1996: Towards a GCM surface parameterization of Amazonia. *Amazonian Deforestation and Climate,* J. H. C. Gash, et al., Eds., John Wiley and Sons, 473–504.

Xue, Y., P. J. Sellers, J. L. Kinter, and J. Shukla, 1991: A simplified biosphere model for global climate studies. *J. Climate,* **4,** 345–364.

Yang, Z.-L., R. E. Dickinson, A. Henderson-Sellers, and A. J. Pitman, 1995: Preliminary study of spin-up processes in land surface models with the first stage data of Project for Intercomparison of Land Surface Parameterization Schemes Phase 1(a). *J. Geophys. Res.,* **100**(D8), 16 553–16 578.

——, Y. Dai, R. E. Dickinson, and W. J. Shuttleworth, 1999a: Sensitivity of ground heat flux to vegetation cover fraction and leaf area index. *J. Geophys. Res.,* **104** (D16), 19 505–19 514.

——, G.-Y. Niu, and R. E. Dickinson, 1999b: Comparing snow simulations from NCAR LSM and BATS using PILPS 2d data. Preprints, *14th Conf. on Hydrology,* Dallas, TX, Amer. Meteor. Soc., 316–319.

Zeng, X., M. Zhao, and R. E. Dickinson, 1998: Intercomparison of bulk aerodynamic algorithms for the computation of sea surface fluxes using TOGA CORE and TAO data. *J. Climate,* **11,** 2628–2644.

——, R. E. Dickinson, A. Walker, M. Shaikh, R. S. DeFries, and J. Qi, 2000: Derivation and evaluation of global 1-km fractional vegetation cover data for land modeling. *J. Appl. Meteor.,* **39,** 826–839.

——, M. Shaikh, Y. Dai, R. E. Dickinson, and R. Myneni, 2002: Coupling of the Common Land Model to the NCAR Community Climate Model. *J. Climate,* **14,** 1832–1854.